

FEDSM-ICNMM2010-30\* ' %

## HIGH STRAIN RATE INDUCED PHENOMENON IN THIN NICKEL FILMS

**Hanif Muhammad Khan**

Division of Mechanical & Automotive  
Engineering,  
College of Engineering, Kongju National  
University, Cheonan 331-717, Republic of Korea  
[hanifmkhan@yahoo.com](mailto:hanifmkhan@yahoo.com)

**Sung-Gaun Kim**

Division of Mechanical & Automotive  
Engineering,  
College of Engineering, Kongju National  
University, Cheonan 331-717, Republic of Korea  
[kimsg@kongju.ac.kr](mailto:kimsg@kongju.ac.kr)

### ABSTRACT

Molecular dynamics study has been performed to investigate the effect of extreme dynamic loading condition on thin Nickel films. Due to the novel aspects of thin films, it has attracted attention over the years for Nano-electro-mechanical systems design. This would be helpful for the analysis of ultra short pulse laser induced fabrication or machining of thin films. Uniaxial high tensile strain namely  $10^9$  and  $10^{10} \text{ s}^{-1}$  has been used on a Nickel thin film. The Embedded-atom method (EAM) potential function for Nickel has been used for the interaction of the atoms. We have observed ductile failure mechanism on both the cases. With the increase of strain rate, not only high strength has been found but also the elastic modulus has been affected less. Random non spherical void growth and their coalescence have been also observed during higher loading condition which leads to a ductile failure mechanism.

### INTRODUCTION

Due to the advancement in Optics, Laser ablation could be used for the fabrication or machining of thin films. The high strain rate induced during ultra short pulsed laser spallation process is of great interest. Several researches have been done to understand the behavior of this kind of process [1-9]. Short laser pulses and ultra short laser pulses induce strain rate exceeding  $10^7 \text{ s}^{-1}$  and  $10^8 \text{ s}^{-1}$  respectively. Such extreme loading condition should be analyzed to understand the phenomenon precisely. Nickel has been chosen as Nickel thin films and Nickel alloys are widely used in Magnetic storage devices and Nano-electro-mechanical-system (NEMS) based technologies. As material size reduces to nano-scale, the

material properties greatly vary from the bulk one which emphasizes the great importance of exploring the nano-scale material property.

### MODELING DETAILS

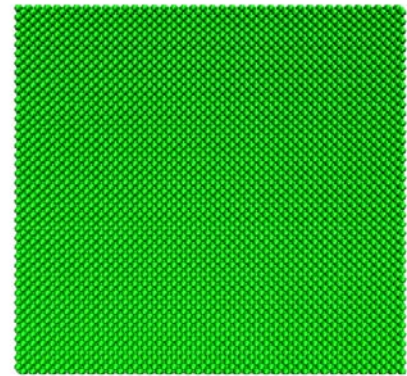


Fig.1: Model of the Thin Nickel Film

Size of the Monocrystalline nickel thin film is  $1.76 \times 14.08 \times 14.08 \text{ nm}$  and contains 35200 atoms which has been illustrated out in Fig.1. The lattice constant of Nickel is  $0.352 \text{ nm}$ . Periodic boundary condition has been maintained in y-direction only. It is also the direction for uniaxial tension test. To incorporate accurate surface phenomenon, other two directions have been maintained as free surface. All models

were subjected to relaxation for equilibrium state at room temperature (300 K) by energy minimization using the conjugate gradient method to allow the models to reach natural and dynamical equilibrium status consistent with the specified temperature. Uniaxial high tensile strain rate such as  $10^9$  and  $10^{10} \text{ s}^{-1}$  has been used on the Nickel thin film to observe the extreme loading condition which has been referred as Case 1 and Case 2 respectively. One end of the thin film has been maintained fixed in its position by maintaining zero forces on the atoms of several layers. Other end of the thin film was subjected to engineering strain by deforming that portion/side with constant velocity. Nose/Hoover thermostat has been used to maintain the temperature and time integration of the atoms to create system trajectory [10-12].

The EAM potential function for nickel developed by Foiles [13] is used here for the interaction of the substrate atoms. The EAM method has been originated from the density-function theory and based upon the approximation that the cohesive energy of a metal is governed not only by the pair-wise potential of the nearest neighbor atoms, but also by embedding energy related to the “electron sea” in which the atoms are embedded. This electron density is approximated by the superposition of atomic electron densities. For EAM potential, the total atomic potential energy of a system is expressed as:

$$E_{tot} = 1/2 \sum_{i,j} \phi_{ij}(r_{ij}) + \sum_i F_i(\bar{\rho}_i) \quad (1)$$

Where  $\phi_{ij}$  is the pair-interaction energy between atoms  $i$  and  $j$  and  $F_i$  is the embedding energy of atom  $i$ .  $\bar{\rho}_i$  is the host electron density at site  $i$  induced by all other atoms in the system, which is given by:

$$\bar{\rho}_i = \sum_{j \neq i} \rho_j(r_{ij}) \quad (2)$$

All the simulations of this model use parallel molecular dynamics program LAMMPS [14]. The discussion provided below is from the careful observations of the MD simulations. For visualization, an open source molecular visualization program namely VMD- Visual Molecular Dynamics has been used [15].

## RESULTS

The stress-strain relationship and corresponding visualizations have been shown on Fig. 2. The reason behind the sudden drop might be due to the undergone phase transformation of the thin film materials which has been also reported by Park et al. [16]. It can be understood from the stress-strain relationship that the possible phase transformation occurs in one step. Further investigation will be focused on this aspect and undergone structure of the thin film will be identified. In Case 1, with the gradual increase of strain, thin film first undergo random spherical void nucleation at almost 23% and it is followed by

void growth and coalescence which is finished at almost 32% strain.

We observed a ductile failure mechanism at almost 60% strain. For case 2, we observed a similar behavior except the nucleation occurs at 30% strain and coalescence occurs at almost 40% strain. The ductile failure mechanism is observed at

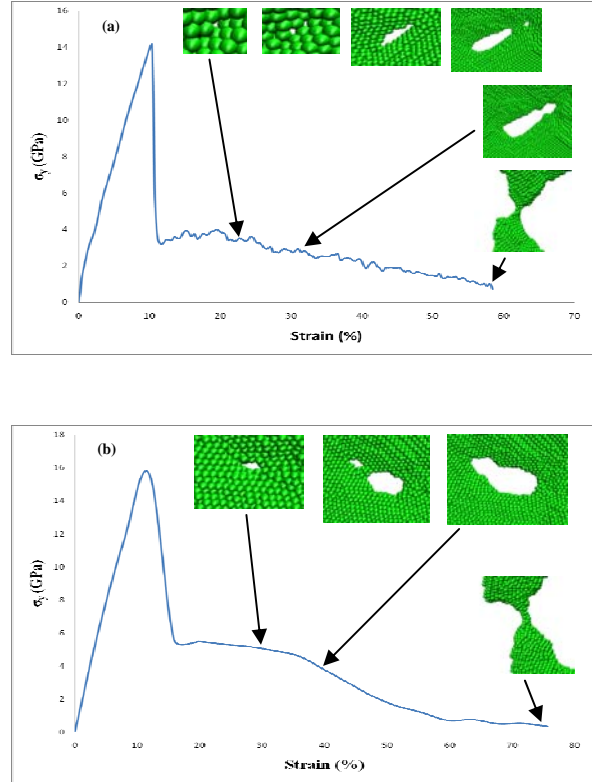


Fig.2: Stress-Strain relation of the Ni thin film at (a) strain rate  $10^9$  and (b)  $10^{10} \text{ s}^{-1}$ .

almost 76% strain. For calculating the elastic modulus, the linear fitted portion up to elastic limit has been used. From the slope of that portion we obtained elastic modulus for Case 1 is 147.8 GPa and for Case 2 is 150 GPa. Obtained yield strengths for Case 1 and Case 2 are 14.14 GPa and 15.62 GPa respectively. The calculated elastic modulus is almost unaffected at both the cases however, the strength of the thin film increases with increased strain rate. Similarly, increase of yield strength with increasing strength rate was also observed in copper nanowires [17]. The discontinuity in elastic-plastic region is totally different from the corresponding bulk material behavior which indicates the detailed analysis of elastic-plastic region for thin films should be taken into consideration for better understanding.

## ACKNOWLEDGMENTS

The authors gratefully acknowledge financial support by Brain Korea 21.

## REFERENCES

- [1] E. Moshe, S. Eliezer, E. Dekel, A. Ludmirsky, Z. Henis, M. Werdiger, I. B. Goldberg, N. Eliaz and D. Eliezer, 1998, "An increase of the spall strength in aluminum, copper, and Metglas at strain rates larger than  $10^7 \text{ s}^{-1}$ ," *J. Appl. Phys.* 83, pp. 4004-4011.
- [2] K. Furusawa, K. Takahashi, H. Kumagai, K. Midorikawa, and M. Obara, 1999, "Ablation characteristics of Au, Ag, and Cu metals using a femtosecond Ti:sapphire laser," *Appl. Phys. A* 69, pp. 359-366.
- [3] M. D. Perry, B. C. Stuart, P. S. Banks, M. D. Feit, V. Yanovsky, and A. M. Rubenchik, 1999, "Ultrashort-pulse laser machining of dielectric materials," *J. Appl. Phys.* 85, pp. 6803-6810.
- [4] H. Tamura, T. Kohama, K. Kondo and M. Yoshida, 2001, "Femtosecond-laser-induced spallation in aluminum," *J. Appl. Phys.* 89, pp. 3520-3522.
- [5] F. Korte, J. Koch and B.N. Chichkov, 2004, "Formation of microbumps and nanojets on gold targets by femtosecond laser pulses," *Appl. Phys. A* 79, pp. 879-881.
- [6] S. Eliezer, I. Gilath and T. Bar-Noy, 1990, "Laser-induced spall in metals: Experiment and simulation," *J. Appl. Phys.* 67 (2), pp. 715-724.
- [7] S. Eliezer, E. Moshe and D. Eliezer, 2002, "Laser-induced tension to measure the ultimate strength of metals related to the equation of state," *Laser and Particle Beams* 20, pp.87-92.
- [8] A.I. Kuznetsov, J. Koch, B.N. Chichkov, 2009, "Nanostructuring of thin gold films by femtosecond lasers," *Appl. Phys. A* 94, pp. 221-230.
- [9] C. Momma, B. N. Chichkov, S. Nolte, F. Alvensleben, A. Tunnermann, H. Welling, B. Wellegehausen, 1996, "Short-pulse laser ablation of solid targets," *Optics Communications* 129, pp. 134-142.
- [10] S. Melchionna, G. Ciccotti, B.L. Holian, 1993, "Hoover NPT dynamics for systems varying in shape and size," *Molecular Physics* 78, pp. 533-44.
- [11] S. Nose, 1984, "A unified formulation of the constant temperature molecular dynamics methods," *J. Chem. Phys.* 81, pp. 511-519.
- [12] W. G. Hoover, 1985, "Canonical dynamics: Equilibrium phase-space distributions," *Phys. Rev. A* 31, pp. 1695-1697.
- [13] S.M. Foiles, M.I. Baskes and M.S. Daw, 1986, "Embedded-atom-method for the fcc metals Cu, Ag, Au, Ni, Pd, Pt, and their alloys," *Phys. Rev. B* 33, pp. 7983-7991.
- [14] S.J. Plimpton and B.A. Hendrickson, 1993, "Parallel molecular dynamics with the embedded atom method." In: Broughton J, Bristowe P, Newsam J, (editors). *Mater. Theory and Modelling*, MRS Proceedings 291 pp. 37.
- [15] W. Humphrey, A. Dalke and K. Schulten, 1996, "VMD: Visual Molecular Dynamics," *J. Mol. Graph.* 14, pp. 33-38.
- [16] H. S. Park, W. Cai, H. D. Espinosa and H. Huang, 2009, "Mechanics of Crystalline Nanowires," *MRS Bulletin* 34, pp. 178-183.
- [17] H. A. Wu, 2006, "Molecular dynamics study of mechanics of metal nanowires at finite temperature," *European Journal of Mech. A/Solids* 25, pp. 370-377.